

Evolutionary Implications from SDSS J085338.27+033246.1: A Spectacular Narrow-Line Seyfert 1 Galaxy with Young Post-starburst

J. Wang¹ and J. Y. Wei¹

National Astronomical Observatories, Chinese Academy of Science

wj@bao.ac.cn

Received _____; accepted _____

Not to appear in Nonlearned J., 45.

ABSTRACT

We analyze the physical properties of post-starburst AGN SDSS J085338.27+033246.1 according to its optical spectrum and discuss its implications on AGN’s evolution. The spectra PCA method is developed to extract emission lines and absorption features from the total light spectrum. The emission-line analysis indicates that the object can be classified as a NLS1 with $\text{FeII}/\text{H}\beta_B = 2.4 \pm 0.2$, large Eddington ratio (~ 0.34), small black hole mass ($\sim 1.1 \times 10^7 M_\odot$) and intermediately strong radio emission. A simple SSP model indicates that the absorption features are reproduced by a ~ 100 Myr old starburst with a mass of $\sim 7 \times 10^9 M_\odot$ rather well. The current SFR $\sim 3.0 M_\odot \text{yr}^{-1}$ inferred from the [OII] emission is much smaller than the past average SFR $\sim 70 M_\odot \text{yr}^{-1}$, however. The line ratio diagnosis using the BPT diagrams indicates that the narrow emission lines are almost entirely emitted from HII regions. We further discuss a possible evolutionary path that links AGN and starburst phenomena.

Subject headings: galaxies: active — galaxies: starburst — quasars: emission lines — quasars: individual (SDSS J085338.27+033246.1)

1. Introduction

In recent years, accumulating evidence supports the hypothesis that AGN reflects an important stage of galaxy formation. Observations reveals the fact that AGN activity and star formation frequently occur together (e.g., Cid Fernandes et al. 2001; Kauffmann et al. 2003; see reviews in Gonzalez Delgado 2002). An important clue of co-evolution of AGN and starburst is the fundamental, tight relationship between mass of supermassive black hole (SMBH) and the velocity dispersion of bulge where the SMBH resides in (e.g., Magorrian et al. 1998; Gebhardt et al. 2000; Tremaine et al. 2002, Greene & Ho 2006). By analyzing the spectra of narrow-line AGNs from Sloan Digital Sky Survey (SDSS, York et al. 2000), Heckman et al. (2004) found that most of accretion-driven growth of SMBH takes place in the galaxy with relatively young stellar population. Recently, as essential relationships relating to AGN’s activity, the Eigenvector 1 space (Boroson & Green 1992, hereafter BG92) was found to be related with ages of the stellar populations as assessed by infrared color $\alpha(60,25)$ (Wang et al. 2006).

It is then natural to ask a question “What is a young AGN?”. Mathur (2000) argued that Narrow-line Seyfert 1 galaxy (NLS1) with high Eddington ratio and small black hole mass might be a young AGN. If so, the co-evolution of AGN and starburst implies that NLS1s are expected to be associated with relatively young stellar populations.

To understand the elusive AGN-starburst connection, we need to carefully examine the properties of AGN’s host galaxy. However, optical spectroscopic study is possible for only a few type I AGNs because the strong nuclear emission usually masks the relatively faint stellar components. By fitting deep off-nuclear optical spectra Canalizo & Stockton (2001) and Nolan et al. (2001) determined the ages of circumnuclear stellar populations for a few IR and optical-selected QSOs respectively. In the happy case, Brotherton et al. (1999) discovered a spectacular “post-starburst quasar” UN J1025-0040 with a ~ 400 Myr

old stellar population. Wang et al. (2004) identified SDSS J022119.84+005628.4 as a NLS1 ($RFe=1.4\pm1.0$) whose spectrum displays a clear Balmer jump. However, the authors did not perform further stellar population analysis.

In this paper, we perform a detailed examination of the physical properties of post-starburst AGN SDSS J085338.27+033246.1 and discuss its implications on study of AGN's evolution. The optical spectrum is extracted from SDSS Data Release 4 (Adelman-McCarthy et al. 2006). Its appropriate spectrum allows us to separate it into a young stellar population and a typical NLS1 spectrum. In addition, the emission line profiles allows us to determine the location on the line ratio diagnostic diagrams. We begin with a brief description of the data reduction in §2. The results and implications are presented in §3. The cosmological parameters: $h = 0.7$, $\Omega_M = 0.3$, and $\Omega_\Lambda = 0.7$ are adopted for calculations.

2. Spectral Analysis

We extract the optical spectrum of SDSS J085338.27+033246.1 when we carry out a systematic search for broad line AGNs from the objects listed in the catalogues¹ released by Kauffmann et al. (2003) and Heckman et al. (2004). Totally hundreds of such objects are extracted from the parent sample. The details of the search and properties of the sub-sample will be presented in subsequent papers. Among these objects SDSS J085338.27+033246.1 has unique properties with strong enough typical AGN spectrum superposed on a spectrum of A-type star. It is coincident that we find the object has been identified as a member of a sample of 74 post-starburst broad line AGNs by Zhou et al. (2005) when our paper is being prepared.

¹These catalogues can be downloaded from <http://www.mpa-garching.mpg.de/SDSS/>.

The observed spectrum is smoothed with a boxcar of 3 pixels ($\sim 5\text{\AA}$) to enhance S/N ratio and precision of the spectra measurements. Standard IRAF procedures are adopted to reduce the raw data, including Galactic extinction correction (with $E(B - V) = 0.048$ from NASA/IPAC Extragalactic Database (NED) and assuming $R_V = 3.1$) and de-redshift to rest frame with $z = 0.207881$. The total light spectrum at rest frame is displayed in Figure 1 (the second line from top to bottom). The spectrum clearly shows a prominent Balmer jump at blue even diluted by an AGN continuum and high order Balmer series.

In the next step, the principal component analysis (PCA) method is developed to remove the stellar light from the observed spectrum (e.g., Li et al. 2005; Hao et al 2005). We build a library of stellar absorption spectra by applying PCA technique on standard SSP models developed by Bruzual & Charlot (2003, hereafter BC03). The first seven eigenspectra are used to model the starlight component by their linear combination. In order to appropriate model the starlight component, our template contains the seven eigenspectra, a power-law continuum, a FeII complex of AGN (adopted from BG92) and a Galactic extinction curve (Cardelli et al. 1989). In order to avoid the distortion of low S/N, a χ^2 minimizing is performed over the rest wavelength range from $\lambda 3700$ to $\lambda 6800$, except for the regions around the strong emission lines. The removal of the stellar component is illustrated in Figure 1 as well. Also plotted are the modeled FeII blends and emission-line spectrum of the AGN. The flux of the FeII blends measured between rest frame wavelength $\lambda 4434$ and $\lambda 4684$ is $(4.23 \pm 0.10) \times 10^{-15}$ ergs s^{-1} cm^{-2} . The detailed comparison between the observed and modeled spectrum at blue is shown in the insert plot A. It is clear that the modeled spectrum reproduces the observed absorption features rather well.

The AGN emission lines are modeled by SPECFIT task as described in Wang et al. (2005, 2006). Briefly, each narrow line (e.g., $\text{H}\alpha$, $\text{H}\beta$, [NII]) is modeled by a Gaussian component. The intensity ratio of [NII] doublets is forced to equal to the theoretical

prediction. The spectra modeling is schemed in the insert plot B and C for H β and H α region, respectively. The upper limit of [OIII] $\lambda 5007$ flux $F(\text{[OIII]}) < 1.2 \times 10^{-16}$ ergs s $^{-1}$ cm $^{-2}$ is estimated by integration rather than fit because the feature is very faint. In addition to these lines, the spectrum displays a broad emission feature at about 5880Å. Based on its asymmetric profile, we identified this feature as HeI $\lambda 5876$ contaminated by broad NaID $\lambda\lambda 5890, 5896$ emission. We find EW(HeI+NaID) $\sim 5.6 \pm 1.3$ Å and (HeI+NaID)/H α_B $= 0.11 \pm 0.02$. The NaID emission was detected in a few AGNs (e.g., Veron-Cetty et al. 2004; Veron-Cetty et al. 2006 and references therein, Thompson 1991). The calculations indicated that the existence of large NaID emission (NaID/H α =0.01-0.05) is related to models with high density ($N_e \sim 10^{11}$ cm $^{-3}$) and large column density ($N_H > 10^{23.5}$ cm $^{-2}$) (Thompson 1991). The measured line properties are summarized in Table 1. The propagation of error is included in the uncertainties shown in parentheses. All the uncertainties given in Columns (2) and (3) are caused by profile modeling.

3. Results and Discussion

3.1. Emission Line Analysis: A NLS1 with Intermediate Strong Radio Emission

According to its spectra properties, we classify SDSS J085338.27+033246.1 as a NLS1 both because of the extremely faint [OIII] emission ([OIII]/H β < 0.05) and because of the relatively narrow H β broad component (FWHM(H β_B)= 1827.6 ± 113.8 km s $^{-1}$). Moreover, the measured RFe is as large as 2.4 ± 0.2 , which is typical of NLS1s.

We further calculate its black hole virial mass and Eddington ratio in terms of the H α broad component according to the equations in Greene & Ho (2005):

$$M_{\text{BH}} = 2 \times 10^6 \left(\frac{L_{\text{H}\alpha}}{10^{42} \text{ ergs s}^{-1}} \right)^{0.55} \left(\frac{\text{FWHM(H}\alpha\text{)}}{1000 \text{ km s}^{-1}} \right)^{2.06} M_{\odot} \quad (1)$$

$$L_{5100} = 2.4 \times 10^{43} \left(\frac{L_{\text{H}\alpha}}{10^{42} \text{ erg s}^{-1}} \right)^{0.86} \text{ erg s}^{-1} \quad (2)$$

The intrinsic luminosity $L(\text{H}\alpha_B) = (2.59 \pm 1.02) \times 10^{42} \text{ ergs s}^{-1}$ is used for calculations because of the large intrinsic extinction $E(B - V) = 0.42 \pm 0.18$. The extinction is calculated from the line ratio $\text{H}\alpha_N/\text{H}\beta_N = 4.8 \pm 1.0$, assuming a Galactic extinction curve and $R_V = 3.1$ (Osterbrock 1989). The inferred virial mass and Eddington ratio is $\sim 1.1 \times 10^7 M_\odot$ and ~ 0.34 , respectively. It is clear that all these properties (i.e., small black hole mass, large RFe value and large Eddington ratio) indicate the object should be potentially classified as a NLS1.

The radio radiation at 1.4GHz of the object was detected by NVSS (Condon et al. 1998) and FIRST Survey (Becker et al. 1995). The map of the FIRST survey shows an unresolved source with a flux $\sim 4.04 \text{ mJy}$ and position $\alpha = 08^{\text{h}}53^{\text{m}}38^{\text{s}}.269$, $\delta = +03^{\circ}32'46''.39$ (J2000). The discrepancy in position given by the optical and radio surveys is much less than $1''$ ($\sim 0''.3$). We determined the extinction-corrected continuum flux that is contributed by AGN at rest wavelength $\lambda 4400$ to be $0.16 \pm 0.02 \text{ mJy}$. If the radio emission is mainly due to AGN, the inferred radio loudness R defined as $R = F_{\text{radio}}/F_{\lambda 4400}$ (Kellermann et al. 1989) is $\log R_{1.4\text{GHz}} = 1.40$ corresponding to $\log R = 1.12$ for 5GHz radio flux². Adopting the division $\log R = 1$ between radio loud and quiet AGN, SDSS J085338.27+033246.1 is an object with intermediately strong radio emission.

We further calculate its radio luminosity $P_{1.4\text{GHz}} \simeq (5.0 \pm 0.3) \times 10^{23} \text{ W Hz}^{-1}$. This luminosity has same order of magnitude of the most radio-luminous starburst ($\log P_{4.85\text{GHz}} \simeq 22.3 - 23.4$, Smith et al. 1998). It has long been known that the decimeter radio luminosity emitted from star-forming galaxy traces supernova rate of massive enough stars (i.e., $M \geq 8M_\odot$). The lifetime of these massive supernova progenitors is $\approx 10^{7.5} \text{ yr}$. The

² $R_{1.4\text{GHz}} = 1.9R_{5\text{GHz}}$ assuming a spectral shape $f_\nu \propto \nu^{-0.5}$ from optical to radio band.

radio supernova itself and its remnant has lifetime ~ 100 yr and $\sim 2 \times 10^4$ yr, respectively. The average SFR over the past $\sim 10^{7.5-8}$ yr therefore relates with the radio emission attributed to supernova as (Condon 1992)

$$\text{SFR}(\geq 5M_{\odot}) = \frac{L_{1.4\text{GHz}}}{4.0 \times 10^{21} \text{ W Hz}^{-1}} M_{\odot}\text{yr}^{-1} \quad (3)$$

For the object, the estimated average SFR is $\sim 70 M_{\odot} \text{ yr}^{-1}$ (see Sect. 3.2 for details). Using a Salpeter IMF (Salpeter 1955), this corresponds to a $\text{SFR}(> 5M_{\odot}) \sim 14M_{\odot} \text{ yr}^{-1}$. The inferred luminosity is therefore $\sim 5.6 \times 10^{22} \text{ W Hz}^{-1}$ and is about one order lower than the total radio luminosity.

3.2. Post-starburst: “A-type star” spectrum and residual star formation

The “A-type star” spectrum indicates the age of the stellar population is no more than a few $\times 10^8$ yrs. To interpret the spectrum of the young stellar population, we extract a series of spectra of SSP models of BC03 with a solar metallicity and with a Chabrier initial mass function. The extracted spectra are matched with the observed spectrum ³ one by one within the wavelength range 3500-5000Å. The spectrum red of $\lambda 5000$ is not used because this part is obviously contaminated by an old population. Figure 2 illustrates the best match between the observed spectrum and a 0.1Gyr old SSP model. The model predicted mass of the starburst is $\sim 7.0 \times 10^9 M_{\odot}$. This simple SSP model shows a past average SFR $\sim 70 M_{\odot}\text{yr}^{-1}$.

However, recent studies suggested that the AGN and starburst activity perhaps not co-evolve simultaneously. Schmitt (2001) suggested that the starbursts may predominate

³In this study the spectrum used for age diagnosis is corrected for intrinsic extinction derived from the PCA modeling.

over AGNs in their earlier phase. Yan et al. (2005) recently suggested that most of SDSS post-starburst galaxies hold somewhat AGN like activities. The post-starburst is the phase in which the galaxy already ceased star formation at some recent epoch. The derived ~ 0.1 Gyr post-starburst in SDSS J085338.27+033246.1 is somewhat similar with the ~ 0.4 Gyr post-starburst that was obtained by Brotherton et al. (1999) in UN J1025-0040.

[OII] $\lambda 3727$ line is widely used as an empirical indicator of ongoing SFR ($\leq 10^7$ yr) for emission line galaxy surveys (e.g., Gallagher et al. 1989; Kennicutt 1992; Hippelein et al. 2003). Its practicability led to several calibrations and a great deal discussions (e.g., Kewley et al. 2004; Kennicutt 1998; Yan et al. 2005). The extinction-corrected flux of [OII] $\lambda 3727$ doublets is $(1.9 \pm 0.7) \times 10^{-15}$ ergs s^{-1} cm^{-2} (with its observed flux shown in Table 1), which yields a ratio $\log([OII]/[OIII]) > 0.55$. Adopting the ratio $\log([OIII]/H\beta_N) < -0.65$, the object is consequently located in the region that represents star formation (Kim et al. 2006 and references therein). It means that the [OII] emission ought to be almost entirely attributed to star formation (see below).

We use the calibration

$$SFR = 7.9 \times \frac{L_{[OII],42}}{16.73 - 1.75[\log(O/H) + 12]} M_{\odot} \text{yr}^{-1} \quad (4)$$

(Kewley et al. 2004) to estimate the SFR, where $L_{[OII],42}$ is the luminosity of [OII] emission in units of 10^{42} ergs s^{-1} . The SFR is inferred to be round about $3.0 M_{\odot} \text{ yr}^{-1}$ by adopting the assumption used in Ho (2005), i.e., the metallicity is twice of solar corresponding to $\log(O/H) + 12 = 9.2$. Here, we obtain a residual but quenched ongoing SFR as obtained in the optically selected QSOs by Ho (2005). The distance-independent birthrate parameter b is defined as the ratio of the current SFR to the average past one (Kennicutt et al. 1994). As a particular case, the object has extremely small value of $b \sim 0.04$, i.e., has present SFR significantly lower than the past.

3.3. Location on the BPT diagram

The traditional BPT diagram (Baldwin et al. 1981) is a powerful tool for diagnosing the origin of emission of narrow lines for emission-line galaxies. The location of the object in the BPT diagram in which the line ratio $[\text{OIII}]/\text{H}\beta$ is plotted against $[\text{NII}]/\text{H}\alpha$ is marked by solid square in Figure 3 (left panel). The solid and dashed line shows the demarcation line between AGN and starburst galaxy defined by Kewley et al. (2004) and Kauffmann et al. (2003), respectively. The figure shows clearly that the position of the object is marginally above the threshold used to define representative HII region. The similar plot is shown in Figure 3 (right panel) but for $[\text{OIII}]/\text{H}\beta$ v.s. $([\text{SII}]\lambda 6719+6731)/\text{H}\alpha$. In this case, the position of the object falls into the region that represents starburst and is far below the demarcation line. The combination of these two diagnosis suggests the observed narrow emission lines are mainly produced by star-formation. What is the distribution in the BPT diagram for post-starburst AGNs is a further interesting question.

3.4. Implications

Here it is interesting to give more discussions on the elusive AGN-starburst connection. Wang et al. (2006) recently indicated that the well-documented E1 sequence most likely represents an evolutionary track of AGN. The track further implies that AGN with high Eddington ratio evolves to one with low Eddington ratio. This result also naturally implies that NLS1s that occupy one extreme end of E1 should be associated with relatively young stellar populations. Apart from the evidence mentioned above, for the IR-selected QSOs, Canalizo & Stockton (2001) found the ages of circumnuclear stellar populations range from current star formation to ~ 300 Myr old. Subsequent spectroscopy studies indicated that about 70%-100% IR-selected QSOs are extremely or intermediately strong FeII emitters (e.g., Lipari et al. 2003; Zheng et al. 2002). Moreover, Zhou et al. (2005) found that more

than half of the post-starburst type I AGN fulfill the criterion for NLS1. All these evidence appear to reveal that a young AGN is most likely a strong FeII emitter with relatively narrow $H\beta$ profile. In contrast, old stellar populations ($\sim 8 - 14$ Gyr) are found to dominate the off-nuclear ($\simeq 5''$) stellar population for optical-selected QSOs (Nolan et al. 2001 and references there in).

These accumulating clues lead us to propose a possible evolutionary scenario that links both AGN and starburst phenomena. The massive starburst might be dominant in the earlier evolutionary phase. Then the starburst passively evolves to A-type stars when the plenty gas falls into the center of a galaxy under the gravitational attraction of SMBH. At one stage about \sim a few $\times 10^8$ yr after the beginning of the starburst, the SMBH begin to accrete matter with small black hole mass and high Eddington ratio. The feedback of the AGN suppresses circumnuclear star formation at the same time (e.g., Kim et al. 2006). The black hole mass grow substantially in the formed bulge in this short phase (e.g. Mathur et al. 2001; Mathur & Grupe 2005). The duration of the phase is commonly estimated as e -folding time scale $t = 4.5 \times 10^7 (\frac{\eta}{0.1}) (\frac{L}{L_{\text{Edd}}})$ yr (Salpeter 1964), where η is the radiative efficiency. The differential growth of AGN and starburst allows the NLS1s below the $M_{\text{BH}} - \sigma_*$ relation for inactive galaxies to approach normal $M_{\text{BH}} - \sigma_*$ relation (Mathur & Grupe 2005; Mathur et al. 2001; Wandel 2002; Bian & Zhao 2004).

The AGN then shines with decreasing accretion rate and insignificantly increasing black hole mass because of the consumption of the gas. The scenario implies that the AGN and host co-evolve marginally around the common $M_{\text{BH}} - \sigma_*$ relation. The luminous AGN phase persists for typical AGN lifetime which is usually believed to be 10^{7-8} yr with however large uncertainties (see reviews in Matini 2004). During this phase, the young stellar population continuously ages and its importance gradually fades. The underlying old stellar population (a few Gyr) finally becomes dominant in the emission of host of an

old AGN. In fact, in addition to the old stellar populations, relatively old post-starbursts (0.1-2Gyr) are frequently detected in off-nuclear regions of a few powerful radio-loud AGNs (e.g. Tadhunter et al. 2005 and references therein). After the luminous phase, AGN then passively evolves to a stage with low luminosity, or low radiative efficiency.

In summary, this scenario could be described as following path: starburst → NLS1+post-starburst → luminous AGN with decreased Eddington ratio+old stellar population → less luminous AGN.

We believe future studies of AGN+post-starburst composite objects such as SDSS J085338.27+033246.1 are important for developing a rational scenario to interpret the AGN-starburst connection.

4. Conclusions

The physical properties of post-starburst AGN SDSS J085338.27+033246.1 are derived by analyzing its optical spectrum. It allows us to obtain results as following. The object can be identified as a NLS1 ($[\text{OIII}]/\text{H}\beta < 0.05$, $\text{FWHM}(\text{H}\beta) = 1827.6 \pm 113.8 \text{ km s}^{-1}$ and $\text{RFe}=2.4 \pm 0.2$) associated with a post-starburst stellar population as identified from the size of the Balmer jump. A simple SSP model indicates the starburst with a mass $7 \times 10^9 M_\odot$ possibly took place $\sim 1.0 \times 10^8 \text{ yr}$ ago. The $[\text{OII}]$ inferred SFR is as small as $\sim 3.0 M_\odot \text{yr}^{-1}$ which is much smaller than the past average one $\sim 70 M_\odot \text{yr}^{-1}$. Its locations in the BPT diagrams show the HII region significantly contributes to the emission of the narrow lines. We further discuss its implications on the elusive AGN-starburst connection.

We would like to thank the anonymous referee for very useful comments and important suggestions. We thank D. W. Xu, C. N. Hao, J. S. Deng and C. Cao for valuable discussions. We are grateful to Todd A. Boroson and Richard F. Green for providing us the FeII

template. This work was supported by the National Science Foundation of China (grant 105030005 and 10473013). This research has made use of the NASA/IPAC Extragalactic Database, which is operated by JPL, Caltech, under contract with the NASA. The SDSS archive data is created and distributed by the Alfred P. Sloan Foundation.

REFERENCES

Adelman-McCarthy, J. K., Agueros, M. A., Allam, S. S., et al., 2006, ApJS, 162, 38

Baldwin, J. A., Phillips, M. M., & Terlevich, R., 1981, PASP, 93, 5

Becker, R. H., White, R. L., & Helfand, D. J., 1995, ApJ, 450, 559

Bain, W., & Zhao, Y., MNRAS, 347, 607

Boroson, T. A., & Green, R. F., 1992, ApJS, 80, 109

Brotherton, M. S., van Breugel, Wil., Stanford, S. A., et al., 1999, ApJ, 520, L87

Bruzual. G., & Charlot. S., 2003, MNRAS, 344, 1000

Canalizo, G. & Stockton, A., 2001, AJ, 555, 719

Cardelli, J. A., Clayton, G. C., & Mathis, J. S., 1989, ApJ, 345, 245

Cid Fernandes, R., Heckman, T., Schmitt, H., et al., 2001, ApJ, 588, 81

Condon, J. J., ARA&A, 30, 575

Condon, J. J., Cotton, W. D., Greisen, E. W., et al., 1998, AJ, 115, 1693

Gallagher, J. S., Hunter, D. A., & Bushouse, H., 1989, AJ, 97, 100

Gebhardt, K., Bender, R., Bower, G., et al. 2000, ApJ, 539, L13

Gonzalez Delgado, R., 2002, ASPC, 258, 101

Greene, J. E., & Ho, L. C., 2005, ApJ, 630, 122

Greene, J. E., & Ho, L. C., 2006, ApJ, 641, L21

Hao, L., Strauss, M. A., Tremonti, C. A., et al. 2005, AJ, 129, 1783

Heckman, T. M., Kauffmann, G., Brinchmann, J., et al., 2004. *ApJ*, 613, 109

Hippelein, H., Maier, C., Meisenheimer, K., et al. 2003, *A&A*, 402, 65

Ho, L. C., 2005, *ApJ*, 629, 680

Kauffmann, G., Heckman, T. M., Tremonti, C., et al., 2003, *MNRAS*, 2003, 346, 1055

Kellermann, K. I., Sramek, R., & Schmidt, M., 1989, *AJ*, 98, 1195

Kennicutt, R. C., 1992, *ApJ*, 388, 310

Kennicutt, R. C., Tamblyn, P., & Congdon, C. E., 1994, *ApJ*, 435, 22

Kennicutt, R. C., 1998, *ARA&A*, 36, 189

Kewley, L. J., Geller, M. J., & Jansen, R. A., 2004, *AJ*, 127, 2002

Kim, M., Ho, L. C., & Im, M., 2006, *astro-ph/0601316*

Li, C., Wang, T. G., Zhou, H. Y., et al. 2005, *AJ*, 129, 669

Lipari, S., Terlevich, R., Diaz, R. J., et al., 2003, *MNRAS*, 340, 289

Magorrian, J., Tremaine, S., Richstone, D., et al., 1998, *AJ*, 115, 2285

Martini, P., 2004, in *Coevolution of Black Holes and Galaxies*, ed., L. C. Ho (Cambridge Univ. Press), 170

Mathur, S., 2000, *MNRAS*, 314, L17

Mathur, S., Kuraszkiewicz, J., & Czerny, B., 2001, *NewA*, 6, 321

Mathur, S., & Grupe, D., 2005, *A&A*, 432, 463

Nolan, L. A., Dunlop, J. S., Kukula, M. J., et al. 2001, *MNRAS*, 323, 308

Osterbrock, D. E., 1989, *Astrophysics of Gaseous Nebulae and Active Galactic Nuclei*, Mill Valley CA: University Science Books

Osterbrock, D. E., & Pogge, R., 1985, *ApJ*, 197, 166

Salpeter, E. E., 1955, *ApJ*, 121, 161

Salpeter, E. E., 1964, *ApJ*, 140, 796

Schmitt, H. R., 2001, *AJ*, 122, 2243

Smith, D. A., Herter, T., & Haynes, M. P., 1998, *ApJ*, 494, 150

Tadhunter, C., Robinson, T. G., Gonzalez-Delgado, R. M., Wills, K., & Morganti, R., 2005, *MNRAS*, 356, 480

Thompson, K. L., 1991, *ApJ*, 374, 496

Tremaine, S., Gebhardt, K., Bender, R., et al., 2002, *ApJ*, 574, 740

Veron-Cetty, M. -P., Joly, M., Veron, P., 2004, *A&A*, 417, 515

Veron-Cetty, M. -P., Joly, M., Veron, P., et al., 2006, *astro-ph/0602239*

Wandel, A., 2002, *ApJ*, 565, 762

Wang, J., Wei, J. Y., & He, X. T., 2004, *ChJAA*, 4, 415

Wang, J., Wei, J. Y., & He, X. T., 2005, *A&A*, 436, 417

Wang, J., Wei, J. Y., & He, X. T., 2006, *ApJ*, 638, 106

Yan, R. B., Newman, J. A., Faber, A. M., et al. 2006, *astro-ph/0512446*

York, D. G., et al. 2000, *AJ*, 120, 1579

Zheng, X. Z., Xia, X. Y., Mao, S., Wu, H., Deng, Z. G., 2002, ApJ, 124, 18

Zhou, H. Y., Wang, T. G., Dong, X. B., Wang, J., Lu, H., 2005, Mem, S. A. It 76, 93

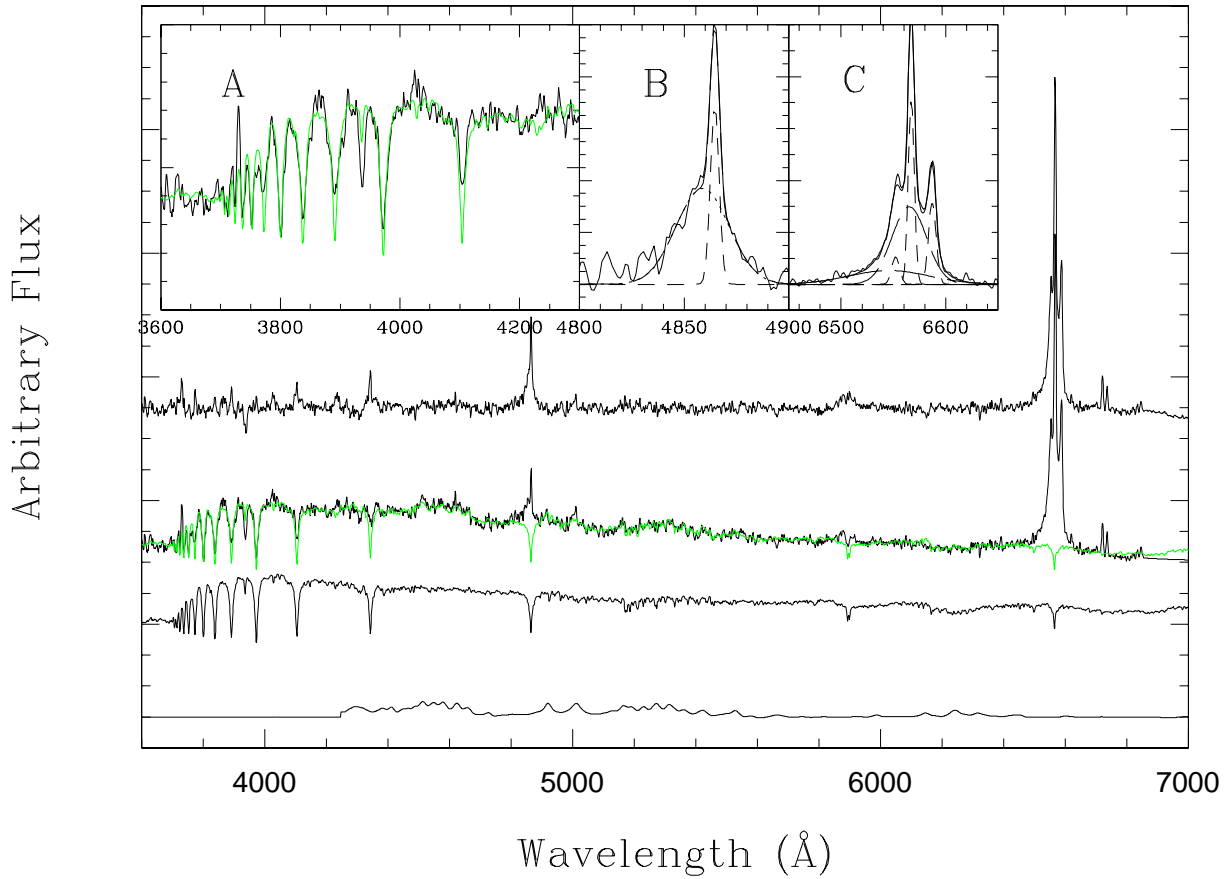


Fig. 1.— Subtracting the stellar component using the linear combination of the 7 eigenspectra and modeling of the emission line profiles. From top to bottom we plot the emission line spectrum, observed spectrum overlaid by the modeled spectrum, modeled spectrum of the host galaxy and modeled FeII blends. The insert plot A shows detailed comparison between the observed and model spectrum at blue. The emission line fit is displayed in the insert plot B and C for H β and H α region, respectively.

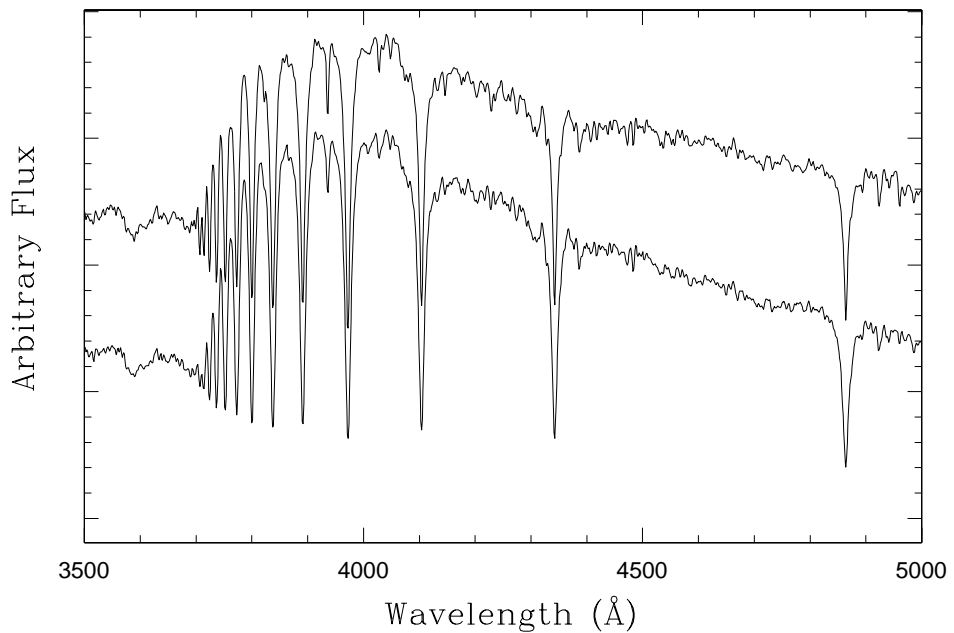


Fig. 2.— An illustration of the match between the stellar spectrum and a 0.1Gyr old SSP model with solar metallicity and Chabrier initial mass function. The SSP model is shifted downward arbitrary for visibility.

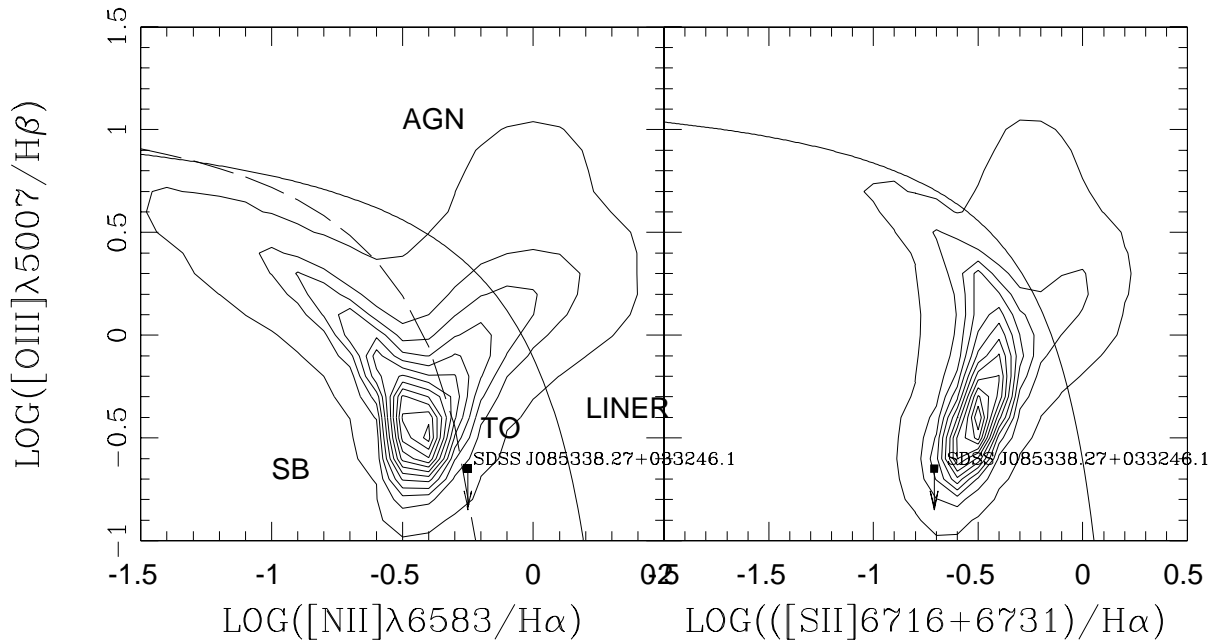


Fig. 3.— *Left panel:* The location of SDSS J085338.27+033246.1 on the BPT diagram defined by line ratio $[\text{OIII}]/\text{H}\beta$ v.s. $[\text{NII}]/\text{H}\alpha$. The density contours are shown for typical distribution of the narrow-line galaxies described in Heckman et al. (2004) and Kauffmann et al. (2003). Only the galaxies with $S/N > 20$ and the emission lines detected at at least 3σ significance are plotted. The solid line is the demarcation line used to separate AGN from starburst by Kewley et al. (2004), and the dashed line by Kauffmann et al. (2003). *Right panel:* The same BPT diagram but for $[\text{OIII}]/\text{H}\beta$ plotted against $([\text{SII}]\lambda 6716 + \lambda 6731)/\text{H}\alpha$.

Table 1: Properties of the emission lines of SDSS J085338.27+033246.1. Flux of each component is normalized to the flux of $H\beta$ narrow component $F(H\beta_N) = (5.4 \pm 0.8) \times 10^{-16} \text{ ergs s}^{-1} \text{ cm}^{-2}$. The uncertainties including propagation of errors are shown in the parentheses.

Line identification	Flux ratio	FWHM (km s ⁻¹)
$H\beta_N$	1.0	301.8 ± 38.0
$H\beta_B$	$3.2 \pm 0.2 (\pm 0.6) \dots$	1827.6 ± 113.8
$[\text{OIII}]\lambda 5007$	$< 0.22 \dots$
$H\alpha_N$	$4.8 \pm 0.4 (\pm 1.4) \dots$	314.9 ± 23.3
$H\alpha_B$	$16.1 \pm 1.1 (\pm 3.1) \dots$	1778.6 ± 150.0
$[\text{NII}]\lambda 6583$	$2.7 \pm 0.3 (\pm 0.6) \dots$	402.2 ± 36.8
FeII 4570	$7.8 \pm 0.2 (\pm 1.4) \dots$
$[\text{OII}]\lambda 3727$	$0.56 \pm 0.02 (\pm 0.10)$
$[\text{SII}]\lambda 6716$	$0.59 \pm 0.06 (\pm 0.12)$	240.2 ± 10.0
$[\text{SII}]\lambda 6731$	$0.35 \pm 0.01 (\pm 0.06)$
HeI+NaID	$1.85 \pm 1.24 (\pm 0.41)$